JOURNAL OF SOLID STATE CHEMISTRY **141,** 10–16 (1998)
ARTICLE NO. SC987882

Chemical Homogeneity of Nanocrystalline Zn–Mn Spinel Ferrites Obtained by High-Energy Ball Milling

D. Arcos,*,† R. Valenzuela,‡ M. Vázquez,†,§ and M. Vallet-Regí*,[1]

*Department of Inorganic and Bioinorganic Chemistry, Facultad de Farmacia, UCM, 28040 Madrid, Spain; †Institute of Applied Magnetism (RENFE-UCM), Las Rozas, Madrid, Spain; ‡Institute for Materials Research, National University of Mexico, Mexico City, Mexico; and §Institute of Materials Science, CSIC, Madrid, Spain

Received January 6, 1998; in revised form April 29, 1998; accepted May 8, 1998

Nanocrystalline Zn–Mn spinel ferrites have been obtained by high-energy ball milling from precursor oxides and carbonates (1) and hydroxides and oxides (2). From the measurement of initial magnetic permeability as a function of temperature, differences in chemical homogeneity have been observed. Structural and Curie point data reveal that dissolution of Mn^{2+} into the spinel structure is assisted by the presence of a hydroxide and an acid oxide. For fixed milling conditions, the influence of precursors leads to different chemical, structural, and magnetic properties in ferrites obtained by mechanochemical synthesis. © 1998 Academic Press

1. INTRODUCTION

Over the last 20 years there has been a considerable interest in solid state mechanochemical processes, ranging from nanocomposites to ceramic oxides (1, 2). In particular the mechanochemical synthesis of spinel ferrites allows the possibility of preparation of magnetic powders with a variety of morphological features, stoichiometry, and phase compositions (3–5). The magnetic and structural properties fall into a wide range depending on several factors like milling time, balls:sample weight ratio, velocities, impact energies, etc. (6, 7).

Nanocrystalline ferrites have been synthesized by mechanical alloying from their starting oxides (8, 9). Other authors have shown that the synthesis of mixed oxides by mechanical milling methods is assisted by the presence of an hydroxide and an acid oxide which results in an acid/base reaction during the milling process (10–12). The use of different precursors also provides new alternatives for the preparation of spinel ferrites.

A serious problem in these synthesis methods is the unavoidable addition of impurities, during milling, leading to chemical inhomogeneity. In turn, this inhomogeneity has strong significant effects on the physical and chemical properties of the resulting material (13). Studies of mechanically treated ferrites with close-packed structural units have shown that, depending on the composition of the close-packed sublattice and on the dimension of cations, energy-intensive grinding leads to various forms of structural failure (14–16).

The initial magnetic permeability is a very microstructure-sensitive property. The study of the thermal variations of initial permeability of polycrystalline ferrites can be used as a quality test in the preparation of ferrite samples (17). At the Curie point the initial permeability falls from a value (generally its maximum) to near 1. The verticality of this drop provides an evaluation of the sample's chemical homogeneity. In this paper, we have used initial permeability measurements as a function of temperature to investigate the chemical homogeneity of our samples.

Our aim is to contribute to the understanding of the problems mentioned above by the study of structure, impurities, and thermal behavior of initial permeability in Mn–Zn ferrites synthesized by mechanical alloying from two different precursors.

2. EXPERIMENTAL

The final product with nominal composition $Zn_{0.40}Mn_{0.56}Fe_{2.04}O_4$ was prepared by high-energy ball milling using two different precursors: (1) oxides and carbonates and (2) hydroxides and oxides. Stoichiometric mixtures of powdered reactants used as starting materials are presented in Table 1. $Fe(OH)_3$ was obtained by precipitation from $Fe(NO)_3$ in high-basicity media and washed until pH 7. α-Fe_2O_3, ZnO, and $MnCO_3$ were Philips Components products, and MnO_2 was a product of Merck.

The milling process was carried out in a Fritsch Pulverisette planetary ball mill at room temperature under air atmosphere. Three grams of the starting materials were

[1]To whom correspondence should be addressed.

0022-4596/98 $25.00

TABLE 1
Composition of Reactant Powders in Weight for Samples Type 1 and Type 2

Precursors	α-Fe_2O_3	$Fe(OH)_3$	$MnCO_3$	MnO_2	ZnO
Type 1 (Oxides and carbonates)	62.84%	—	24.78%	—	12.38%
Type 2 (Hydroxides and oxides)	—	73.16%	—	16.32%	10.52%

sealed in a stainless steel vial (45 cm^3 in volume) together with chromium-tempered stainless steel balls 15 mm in diameter. The ball-to-powder weight ratio was 25:1. About 11 h were required to obtain the spinel phase with both kinds of precursors. Powder ferrites weighing 0.5 g were pressed into toroids 9 mm o.d. 5 mm i.d., and 2 mm thick under 2 tons cm^{-2} for 2 min. Since heating at 650°C in air leads to the decomposition of the spinel structure into hematite and the other starting oxides, thermal treatments were carried out in argon atmosphere at 650°C, with a heating rate of 20°C min^{-1}, and then quenched in air.

Scanning electron micrographs of the investigated samples were taken on a Leica scanning electron microscope (SEM) using an acceleration voltage of 20 kV. The compositional analysis of different areas of the samples was carried out by an energy dispersion X-ray (EDX) analyzer. EDX intensities were converted to the relative concentrations.

X-ray diffraction patterns were collected using a Siemens D-5000 diffractometer with Cu$K\alpha$, and differential scanning calorimetry (DSC) was carried out using a Perkin-Elmer DSC-7 calorimeter. DSC experiments were carried out under the same conditions as the heating of the samples.

FTIR spectrometry were measured using a Nicolet Magna-IR spectrometer 550.

The apparatus for the measurement of initial magnetic permeability as a function of temperature comprises a low-frequency signal generator (General Radio 1310), a voltage amplifier and rectifier (Philips 5171), and an X–Y recorder (Hewlett-Packard HP 7035). The signal from the secondary coil is amplified, rectified, and recorded on the Y axis of the plotter. The temperature signal is provided by a thermocouple in contact with the sample and connected to the X-axis of the recorder. The frequency was set to 10 kHz, the primary coil to 6 turns, and the primary current level to 1 mA. This apparatus is explained elsewhere (18).

3. RESULTS AND DISCUSSION

Scanning electron micrographs of samples type 1 and type 2 (Fig. 1) show a mixture of individual particles with diameter of about 0.2 μm and aggregates with very different size.

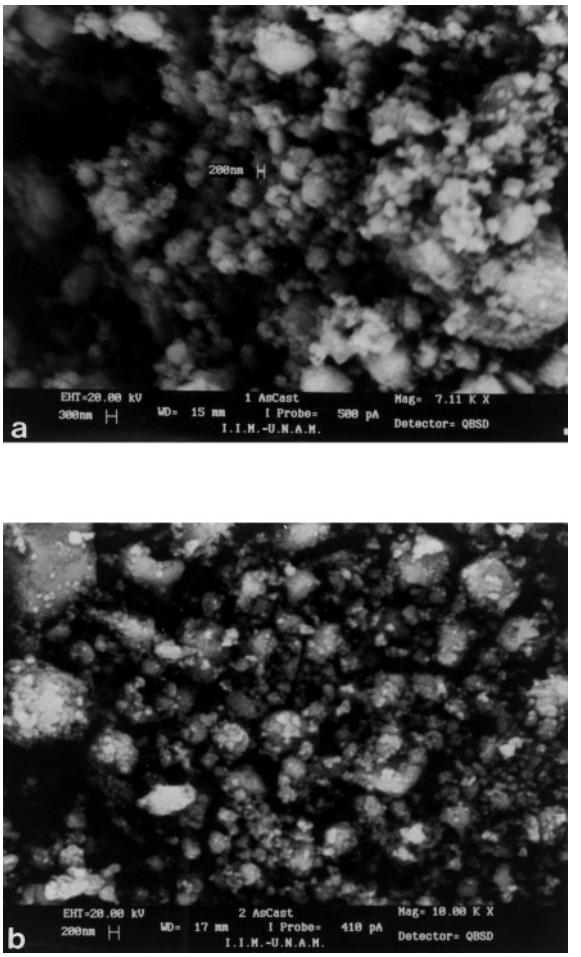

FIG. 1. Scanning electron micrographs of samples (a) type 1 and (b) type 2.

In Table 2 we show the composition of samples type 1 and type 2 observed by the EDX experiment, pointing out the variation that both samples show when the experiment

TABLE 2
Relative Compositions in Weight Obtained by EDX Spectroscopy[a]

Sample	Zn%	Mn%	Fe%	O%	Cr%
Type 1	11.02 (±5%)	11.12 (±2%)	48.54 (±7%)	28.43 (±4%)	0.89
Type 2	9.45 (±3%)	10.84 (±3%)	49.73 (±7%)	29.25 (±7%)	2.15
Theoretical composition	11.13	13.10	48.52	27.25	—

[a]Percentage in brackets refer to the chemical variation observed when the experiment is carried out over different areas.

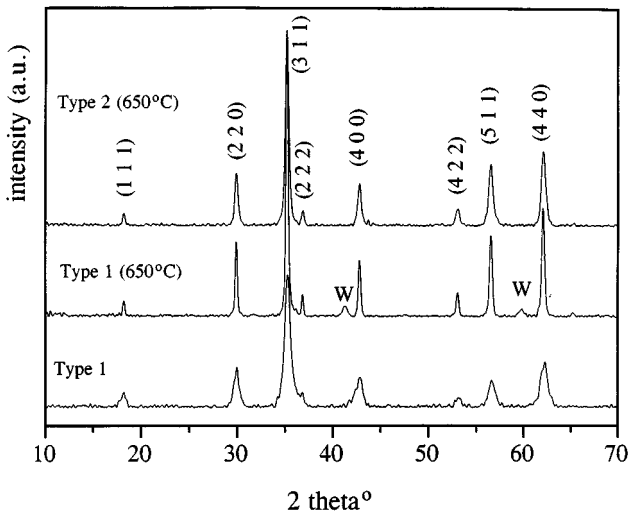

FIG. 2. XRD patterns for samples type 1, type 1 (650°C), and type 2 (650°C). Indices for spinel structure are indicated and (W) corresponds to wűstite phase. Sample type 2 showed a XRD pattern similar to sample type 1.

In order to study the thermal behavior of these ferrites, we submitted both samples to thermal treatment under argon atmosphere. The heating rate was 20°C min^{-1} until 650°C, and then the samples were quenched in air in order to avoid the subsequent grain growth. Scanning electron micrographs show images similar to those obtained from ferrites without heating, that is to say, a mixture of individual particles (of about 0.2 μm) with agglomerates of different size (Fig. 3). No particle growth seems to have occurred.

However, XRD patterns after thermal treatment show a relaxed single spinel phase in the case of sample type 2, 650°C annealed, and a relaxed spinel phase together with a segregated wüstite phase in the case of sample type 1, 650°C annealed (Fig. 2). In Table 3 we show the structural parameters of both mechanochemical synthesized ferrites and their corresponding annealed samples.

Table 3 data reveal that synthesis of spinel ferrites by high-energy ball milling leads to nanocrystalline structures with metastable thermal behavior. The lattice parameter of a sample of the same nominal composition synthesised by

is carried over two different contrast areas observed on SEM micrographs. The degree of chromium contamination from the balls is also shown.

EDX spectroscopy shows important chemical differences in both samples. Deviations from the nominal composition in different areas show the high degree of chemical inhomogeneity in particles and aggregates.

The excess in oxygen content can be explained by the presence of unreacted starting oxides. Moreover, samples obtained from an hydroxide and an acid oxide (type 2) led to a higher degree of chromium impurities (more than twice) with respect to samples type 1. In this way, the higher Fe content in sample type 2 compared to the theoretical composition could be due to Fe from the balls. This data can be explained by the acid/base reaction assisting to the mechanochemical synthesis, which leads to a higher corrosion on the surface on the chromium tempered stainless steel balls.

XRD patterns of both samples (Fig. 2) show that nanocrystalline spinel ferrites were obtained. The broad shape of the diffraction maxima reflects the formation of the disordered structure, with small crystallite size (8–17 nm) and with strong internal strains introduced by the mechanical treatment. Crystallite size was measured Debye–Scherrer method. Previously, Gaussian deconvolution of the diffraction maxima were carried out. Since from the method mentioned above it is not possible to separate the contribution of the strains (induced by the milling) over the FWMH of the diffraction maxima, it must be noted that with "crystallite size" the authors refer to the average size of coherent domains of diffraction, which involve these two contributions.

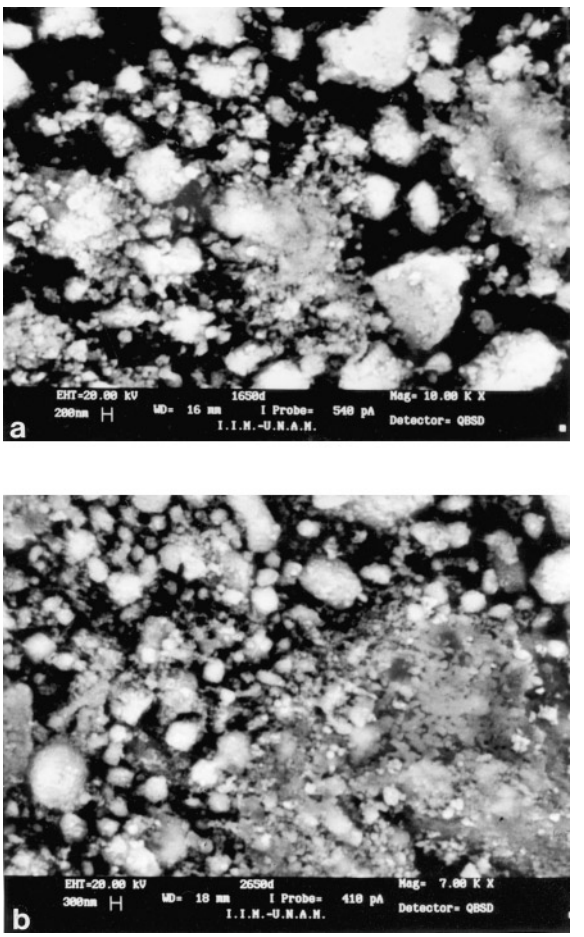

FIG. 3. Scanning electron micrographs of samples (a) type 1 (650°C) and (b) type 2 (650°C).

TABLE 3
Structural Parameters Obtained from XRD Patterns for Zn–Mn Ferrites Synthesized from Type 1 and 2 Precursors and Their Corresponding 650°C Annealed Samples

Sample	Type 1	Type 1, 650°C annealed	Type 2	Type 2, 650°C annealed
Lattice parameter (Å)[a]	8.4496	8.4401	8.4482	8.4665
Crystallite size (Å)	127	508	101	396

[a]Lattice parameter of the same nominal composition synthesized by the conventional ceramic method showed values of 8.4650 Å.

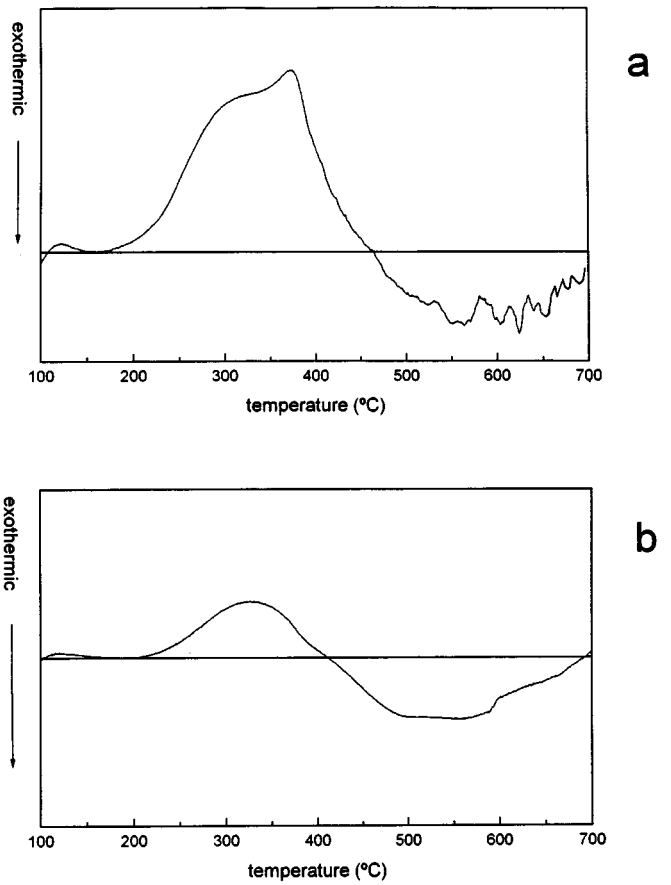

FIG. 4. DSC diagrams of samples (a) type 1 and (b) type 2.

the conventional ceramic method shows a value of 8.4650 Å. So, we can say that lattice contraction occurs with respect to ceramic Zn–Mn ferrite. That is in agreement with the idea that during mechanical treatment a partial deformation of the anion sublattice takes place, although cubic symmetry with space group *Fd3m* is maintained (14). In addition, we think that a noncomplete and inhomogeneous cation dissolution in spinel structure takes place. It would lead to vacancies in cation sublattice (especially because of a greater cation such as Mn^{2+} into tetrahedral sites) as we reported elsewhere (19), which would contribute to lattice contraction.

Structural data of samples annealed show differences related with the type of precursor used in the mechanochemical synthesis. In ferrites type 1 (650°C), the segregation of a second phase (wüstite) leads to a higher contraction of the lattice parameter. This segregation occurs when samples type 1 are quenched in air. It shows the metastability and the noncomplete cation dissolution into the spinel structure (even after thermal treatment) in ferrities synthesized by this first way. For sample type 2 (650°C), the XRD pattern shows a relaxed single spinel phase. Heating leads to an enhanced lattice parameter which points out that thermal treatment under argon atmosphere assists the cation dissolution into the spinel structure.

In Fig. 4 DSC diagrams show a set of endothermic processes between 180 and 400°C that involve the reaction of small amounts of unreacted raw materials and gas desorption. This reaction requires much lower temperature, compared to ordinary solid state reaction, due to the instability and high specific surface of the sample. From the heating rate and the area under curve where processes occurred, we calculate energies of about 20 and 7 kJ mol^{-1} for samples of type 1 and type 2, respectively, from the endothermic processes observed in DSC experiment. Exothermic processes are observed between 450 and 700°C for sample type 1 and between 400 and 700°C for type 2. The released heat corresponds to the energy stored in the mechanically distorted structure, which is about 12 and 10 kJ mol^{-1} for samples type 1 and type 2, respectively. DSC experiments agree with a high-stressed and low-crystalline phase to a more crystalline phase transition, obtained after structural relaxation by means of heating. These data agree with the obtained by XRD (Fig. 2).

IR spectra of sample type 1 are presented in Fig. 5. In the spectra, band at 1400 cm^{-1} correspond to the vibrational modes of CO_3^{2-} groups. In addition, vibrational modes at 3375 cm^{-1} from the H_2O adsorbed can also be observed. The presence of a band at 1625 cm^{-1} indicates the existence of M–OCO_2 and/or M–OH_2 as intermediate reactives.

Measurement of Initial Magnetic Permeability

It is now well accepted (20–22) that initial magnetic permeability depends essentially on the ratio M_s^2/K_1, where is the M_s saturation magnetization value and K_1 is the magnetocrystalline anisotropy constant. The thermal variations of μ_i should therefore correspond to the thermal variations

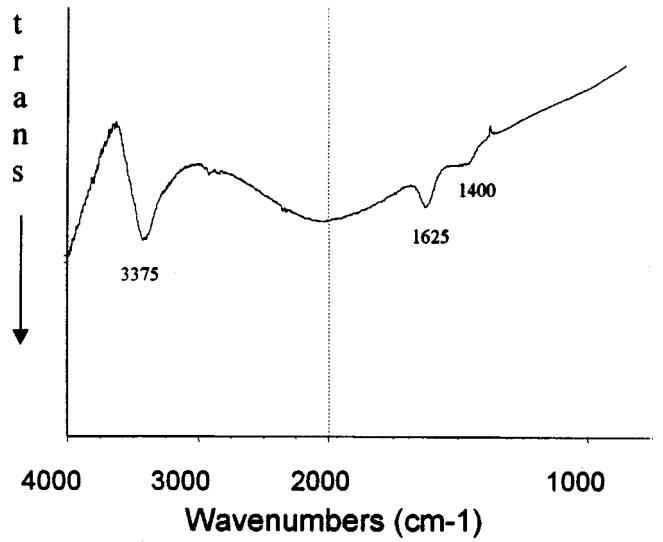

FIG. 5. IR spectra of sample type 1.

of M_s^2/K_1. In most of the cases the saturation magnetization of ferrites decreases slowly with temperature, while their anisotropy constant decreases much more rapidly. Initial permeability shows therefore an increase with temperature which grows more rapidly as T increases, as widely observed experimentally. At the Curie point, the initial permeability drops from its maximum value to the value corresponding to the paramagnetic phase, i.e., typically close to 1. Since the Curie temperature value depends essentially on the superexchange interactions in the ferrite (23), and therefore on its composition, any inhomogeneity in the composition leads to a nonunique transition temperature. In a schematic way, chemical inhomogeneities produce a sample with more than one Curie point.

Zn-mixed ferrites of general formula $Zn_xM_{1-x}Fe_2O_4$, where M is a divalent cation such as Ni, Mn, Co, or Fe^{2+}, form complete solid solution series. Accordingly, their properties, in particular the Curie temperature, show a continuous variation with Zn content x. For samples of these ferrites obtained from the corresponding oxides by the classic ceramic method, it is a well-known problem to attain an acceptable degree of chemical homogeneity with short sintering times. If, as a result of an incomplete sintering process the ferrite grains possess a composition gradient, their Curie temperature, as observed by means of the initial permeability exhibits a drop encompassing a considerable temperature range (17).

The variations in the Curie temperature value of ferrites has been investigated for compressive pressures up to 1200 bar (24). Within the experimental error limits, T_C has shown to be independent of stress.

The initial magnetic permeability (μ_i) of synthesized ferrites and their corresponding 650°C annealed samples was measured up to the Curie point. Curves of μ_i for samples of types 1 and 2, Fig. 6, showed a very low value of initial permeability. Also, the observed magnetic transition from the ordered ferrimagnetic phase toward the disordered paramagnetic phase encompass a large temperature range (~ 150 and ~ 112 K for samples of types 1 and 2, respectively). From the above paragraphs, both samples must be considered, as having a very high chemical inhomogeneity, i.e., there exists a wide distribution of Curie temperatures within the sample.

Differences in the behavior of μ_i between ferrites type 1 and 2 are observed. While values of initial permeability are similar in both ferrites the temperature at which the highest values (Curie point) are reached varies significantly (393 and 448 K for ferrites type 1 and type 2 respectively).

The difference in the Curie temperature between both samples is due to the composition of the magnetic component. As zinc content is increased, the magnetic interactions decrease and the long-range order is broken at lower temperatures. In the Zn–Mn ferrites Curie temperature varies according to the composition from 573 K for $MnFe_2O_4$ to about 533 K for $Zn_{0.5}Mn_{0.5}Fe_{2.0}O_4$ (21). Curves of μ_i as a function of temperature show that precursors type 2 assist the dissolution of Mn^{2+} into the spinel structure with respect to precursors type 1. This is clear from the higher chemical homogeneity that shows the drop at the Curie point for sample type 2 as well as the higher Curie temperature which point out a higher Mn:Zn ratio into the magnetic component. Since magnetite (Fe_3O_4) has a T_C of 854 K, samples exhibiting a Curie temperature drop at $T > 573$ K contain some Fe^{2+}.

Not only homogeneity is enhanced when precursor type 2 are used; XRD patterns showed that for annealed samples, the thermal stability of the spinel structure is also enhanced. Heating ferrites type 1 leads to a partial decomposition of spinel structure, segregating a wüstite phase, with the subsequent decreasing of the spinel lattice parameter. Annealing at 650°C in argon atmosphere of ferrites type 2 lead to an almost single spinel phase, introducing the unreacted starting oxides with the subsequent enhancement of the lattice parameter.

The effect of annealing on initial permeability is shown in Fig. 7. It is clear from these curves that a homogenization process takes place. The Curie point is increased in both samples (498 and 543 K for type 1 (650°C) and type 2 (650°C), respectively) as well as the verticality of the drop at this point (within ± 29 and ± 35 K for annealed samples type 1 and type 2, respectively), which show the dissolution of Mn^{2+} into the spinel structure.

We think that the lower Curie point of sample type 1 (650°C) with respect to type 2 (650°C) is a consequence of Mn segregation into wüstite structure with the subsequent

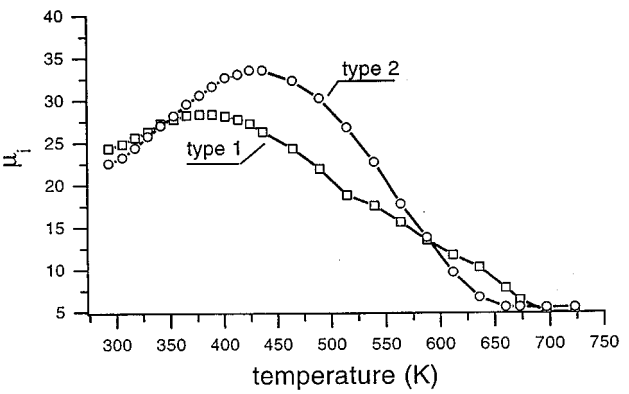

FIG. 6. Initial magnetic permeability of samples type 1 and type 2.

decreasing of Mn:Zn ratio in the spinel. Lattice parameter of 4.363 Å was calculated for the segregated wüstite phase, while this value is 4.307 Å for wüstite of nominal composition FeO. Taking into account the higher volume of Mn^{2+} with respect to the Fe^{2+} (ratios of 0.80 and 0.77 Å, respectively), we think the segregated phase corresponds to a composition $(Fe_{1-x}Mn_x)O$.

On the other hand, the enhanced μ_i value in type 1 (650°C) is in agreement with the larger crystallite size measured by XRD (Table 3).

4. CONCLUSIONS

Synthesis of Zn–Mn ferrites with spinel structure by high-energy ball milling leads to metastable nanocrystalline spinel ferrites. These ferrites have a high degree of inhomogeneity due to the deficient dissolution of the larger cations such as Mn^{2+} into the structure. This chemical inhomogeneity can be reduced by using hydroxides and acid oxides as precursors, as alternatives to oxides and carbonates, since an acid/base reaction assists the dissolution of Mn^{2+}, leading to more stable phases. On the other hand, the acid/base reaction performed during the mechanical treatment leads to a higher powder contamination from the balls.

Finally, the relation between Zn:Mn ratio and Curie point as well as the drop of permeability at this point with the chemical homogeneity makes the measurement of initial magnetic permeability as a function of temperature an excellent qualitative tool in the study of chemical homogeneity for mechanochemically synthesized Zn–Mn spinel ferrites.

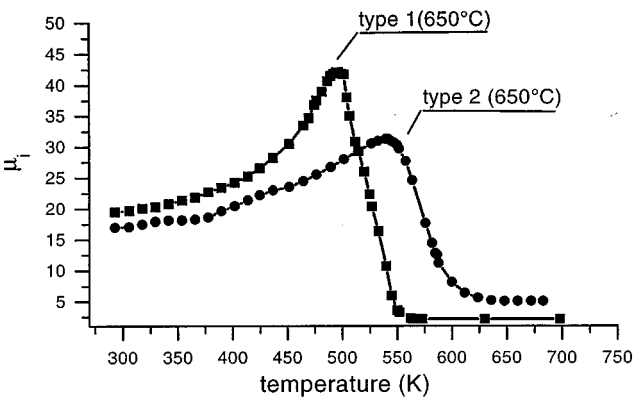

FIG. 7. Initial magnetic permeability of samples type 1 (650°C) and type 2 (650°C).

ACKNOWLEDGMENTS

This work was partially supported by CICYT-Spain, Research Project MAT 96-0919, The European Commission, St. Andrews Materials ALFA Network, and DGAPA-UNAM Mexico, Grant IN 100996. The authors thank J. Guzman for technical assistance with the SEM.

REFERENCES

1. S. Linderoth and M. S. Pedersen, *J. Appl. Phys.* **75,** 5867 (1994).
2. Gaffet, D. Michel, L. Mazerolles, and P. Berthet, *Mater. Sci. Forum* **235–238,** 103 (1997).
3. W. A. Kacmarek and B. W. Ninham, *IEEE Trans. Magn.* **MAG-30,** 732 (1994).
4. W. A. Kacmarek, *Mater. Sci. Forum* **235–238,** 109 (1997).
5. W.A. Kacmarek, I. Onyszkiewicz, and B. W. Ninham, *IEEE Trans. Magn.* **MAG-30,** 4725 (1994).
6. P. G. McCormick, H. Huang, M. P. Dallimore, J. Ding, and J. Pan, "Proceedings of the 2nd International Conference of Structural Applications of Mechanical Alloying," Vancouver, Canada, September 20–22, 1993.
7. M. P. Dallimore and P.G. McCormick, *Mater. Trans.* **37,** 1091 (1996).
8. J. Ding, T. Reynolds, W. F. Miao, P. G. McCormick, and R. Street, *Appl. Phys. Lett.* **65,** 3135 (1994).
9. C. Suryanarayana, "Bibliography on Mechanical Alloying and Milling." Cambridge Int. Science Publishing, Cambridge, 1995.
10. J. G. Baek, K. Gomi, T. Watanabe, T. Isobe, and M. Senna, *Mater. Sci. Forum* **235–238,** 115 (1997).
11. T. Watanabe, J. Liao, and M. Senna, *J. Solid State Chem.* **115,** 390 (1995).
12. T. Watanabe, T. Isobe, and M. Senna, *J. Solid State Chem.* **122,** 74 (1996).
13. M. Seidel, J. Eckert, and L. Shultz, *Mater. Sci. Forum* **235–238,** 121 (1997).
14. V. Sepelák, K. Tkácová, V. V. Boldyrev, and U. Steinike, *Mater. Sci. Forum* **228–231,** 783 (1996).
15. Yu. T. Pavlyukhin, Ya. Ya. Medikov, and V. V. Boldyrev, *J. Solid State Chem.* **53,** 155 (1984).
16. K. Tkácová, V. Sepelák, N. Stevulová, and V. V. Boldyrev, *J. Solid State Chem.* **123,** 100 (1996).
17. A. Globus and R. Valenzuela, *IEEE Trans. Magn.* **MAG-11,** 1300 (1975).

18. E. Cedillo, J. Ocampo, V. Rivera, and R. Valenzuela, *J. Phys. E*: *Sci. Instrum.* **13,** 383 (1980).
19. D. Arcos, N. Rangavittal, M. Vazquez, and M. Vallet-Regí, *Mater. Sci. Forum* **269–272,** 87 (1998).
20. M. Kersten, *Z. Angew. Phys.* **8,** 382 (1956).
21. T. Merceron and J. L. Dormann, *J. Magn. Magn. Mater.* **15–18,** 1435 (1980).
22. R. Aragón, D. J. Buttrey, J. P. Shepherd, and J. M. Honig, *Phys. Rev. B* **31,** 430 (1985).
23. R. Valenzuela, "Magnetic Ceramics." Cambridge Univ. Press, Cambridge, 1994.
24. M. LeFloch, J. Loaec, and A. Globus, *J. Magn. Magn. Mater.* **15–18,** 1437 (1980).
25. K. Ohta, *J. Phys. Soc. Jpn* **18,** 865 (1963).